Ground Clutter Canceling with a Regression Filter

SEBASTIÁN M. TORRES

Cooperative Institute for Mesoscale Meteorological Studies, Norman, Oklahoma

DUSAN S. ZRNIC

NOAA/ERL/National Severe Storms Laboratory, Norman, Oklahoma

(Manuscript received 10 September 1998, in final form 4 January 1999)

ABSTRACT

This paper explores ground clutter filtering with a class of cancelers that use regression. Regression filters perform this task in a simple manner, resulting in similar or better performance than the fifth-order elliptic filter implemented in the WSR-88D. Assuming a slowly varying clutter signal, a suitable projection of the composite signal is used to notch a band of frequencies at either side of zero Doppler frequency. The complexity of this procedure is reduced by using a set of orthogonal polynomials. The frequency response of the resulting filter is related to the number of samples in each input block and the maximum order of approximating polynomials. Through simulations, it is demonstrated that the suppression characteristic of this filter is better than that of step-initialized infinite impulse response filters, whereby transients degrade the theoretical frequency response. The performance of regression filters is tested with an actual weather signal, and their efficiency in ground clutter canceling is demonstrated.

1. Introduction

Weather radar data are often contaminated with unwanted returns from the ground. Therefore, filtering techniques that attempt to ameliorate these signals are essential in nearly all Doppler radar systems. If the clutter is not at least partially removed, it can mimic a meteorological signal and might produce strongly biased estimates of the three fundamental physical parameters (mean power, mean Doppler velocity, and spectrum width). In most cases, ground clutter signals have a narrow spectrum width (long correlation time) compared with weather signals, and their mean Doppler velocity is zero. Thus, a high percentage of this interfering signal can be reduced if the spectral components in a band centered at zero frequency (zero Doppler velocity) are removed by a suitable high-pass filter. Ground clutter filters (GCFs) with sharp narrow notches have been successfully designed and implemented in the WSR-88D to operate on pulse trains with uniformly spaced pulses, that is, uniform pulse repetition time (PRT) (Heiss et al. 1990).

In this paper we address the issue of ground clutter elimination with regression filters. Besides being easily designed and implemented, these filters can be directly extended to signals that are nonuniformly sampled. First, some concepts of clutter filtering are presented with particular emphasis on implementation of such filters using regression. Once the design variables are described and analyzed, the regression filter performance is assessed. This is accomplished by studying statistical properties of spectral moments of simulated weather signals to which ground clutter is superposed. Finally, a regression filter and a recursive filter designed for the Next Generation Weather Radar (NEXRAD) are applied to a time series of actual weather echoes and ground clutter collected by an operational WSR-88D.

2. Regression ground clutter filter

Ground clutter filters are high-pass filters that ideally remove frequency components at either side of zero Doppler velocity and leave the rest of the spectrum almost intact. It is very important to recognize this property during the design phase because any changes in the magnitude response will directly bias the estimates of the three parameters of interest. On the other hand, it is relatively easy to prove that the phase characteristic of the filter is immaterial. To observe this, recall that power, mean velocity, and spectrum width estimates depend on the estimated autocorrelation function of the filtered weather signal. It is well known that the power spectral density (PSD) of the output of a linear time-

Corresponding author address: Sebastian M. Torres, NSSL, 1313 Halley Circle, Norman, OK 73069.
E-mail: sebastian.torres@nssl.noaa.gov

invariant filter $S_y(\omega)$ is related to the PSD of the input $S_x(\omega)$ by the magnitude square of the frequency response of the filter, $|H(\omega)|^2$. That is,

$$S_y(\omega) = S_x(\omega)|H(\omega)|^2. \tag{1}$$

Moreover, the autocorrelation function is uniquely determined by the corresponding PSD through a Fourier transform pair relation. Because the phase response of the filter is not involved in this transformations, it has no effect on the autocorrelation of the filter output weather signal.

Here we investigate suitability of regression filters for ground clutter suppression and compare their performance to the fifth-order elliptic infinite impulse response (IIR) ground clutter filters implemented in the WSR-88D. Application of regression filters to clutter suppression in Doppler ultrasonic blood flow meters was presented by Hoeks et al. (1991) and extended by Kadi and Loupas (1995) and Torp (1997) in the context of a uniform PRT. Application of the first-order regression GCF to wind profiling radars was demonstrated by May and Strauch (1998).

Classic digital filters can be divided into two classes: finite impulse response and infinite impulse response filters. For either class, filtering is achieved by superposition of signal samples. Unlike these filters, regression filters utilize projections of elements from the signal vector space S onto the clutter signal subspace W of S. These projections can be efficiently performed if W is described by an orthogonal basis B. However, orthogonality alone is not sufficient to completely specify this basis. To improve the computational efficiency of this filtering process, we can limit the functions in B to polynomials over a set of discrete points on the real line. Orthogonal polynomials have received much attention in applications such as rational interpolation, least squares polynomial approximation, and smoothing of nonlinear functions. Egecioglu and Koc (1992) presented an efficient algorithm to generate such polynomials over an arbitrary set of points $\{t_m\} = \{t_0, t_1, \ldots, t_{M-1}\}$.

Regression filters approximate their input signals with polynomial functions in the time domain, and their design is not based on traditional tools such as the impulse or frequency responses. The clutter signal varies slowly compared to the weather echo signal and consequently can be approximated with a polynomial of a relatively low degree. This approximation is usually performed using least squares methods or the equivalent transformation, which projects the input signal samples $V(t)$, $t \in \{t_m\}$ onto the subspace W spanned by a basis B consisting of $p + 1$ orthonormal polynomials. This set of polynomials is given by $B = \{b_0(t), b_1(t), b_2(t), \ldots, b_p(t)\}$, where each $b_i(t)$ $(0 \le i \le p)$ is a polynomial of ith degree; that is, $b_i(t) = c_{0i} + c_{1i}t + \cdots + c_{ii}t^i$. Then, the projection $\hat{V}(t)$ (i.e., the clutter signal) is obtained by constructing a linear combination of the elements of the basis B, that is, the implication is that $\hat{V}(t)$ is in W and, therefore,

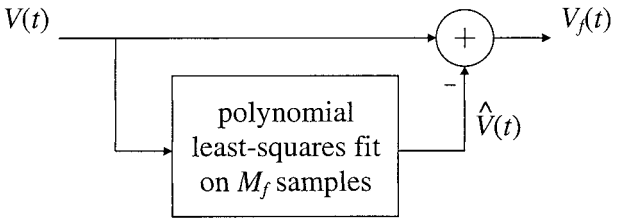

FIG. 1. Regression filter block diagram. Signals are processed in overlapping blocks of M_f samples each.

$$\hat{V}(t_m) = \sum_{i=0}^{p} \alpha_i b_i(t_m). \tag{2}$$

Accordingly, the residue $V_f(t_m) = V(t_m) - \hat{V}(t_m)$ is associated with the portion of the input signal that is not contained in the clutter subspace W [i.e., it is orthogonal to $\hat{V}(t)$]. The α_i coefficients are computed using the classical formula (Papoulis 1986, 146–154)

$$\alpha_i = \frac{(\mathbf{V}, \mathbf{b}_i)}{\|\mathbf{b}_i\|^2} = \frac{\sum_{m=0}^{M-1} V(t_m) b_i(t_m)}{\sum_{m=0}^{M-1} b_i^2(t_m)} \qquad i = 0, 1, \ldots, p, \tag{3}$$

where $\mathbf{V}$ and $\mathbf{b}_i$ are vectors of the sampled input signal and the $b_i(t)$ polynomials, respectively.

Generalization in this analysis is not lost if each element of B is normalized such that $\|\mathbf{b}_i\| = 1$, where $\|\mathbf{b}_i\|^2 = (\mathbf{b}_i, \mathbf{b}_i)$. In addition, to simplify the notation define the basis matrix $\mathbf{B}$ and the coefficient vector $\mathbf{A}$ as

$$\mathbf{B} = \begin{bmatrix} b_0(t_0) & b_0(t_1) & \cdots & b_0(t_{M-1}) \\ b_1(t_0) & b_1(t_1) & \cdots & b_1(t_{M-1}) \\ \vdots & \vdots & \ddots & \vdots \\ b_p(t_0) & b_p(t_1) & \cdots & b_p(t_{M-1}) \end{bmatrix} \quad \text{and} \quad \mathbf{A} = \begin{bmatrix} \alpha_0 \\ \alpha_1 \\ \vdots \\ \alpha_p \end{bmatrix}. \tag{4}$$

Then, assuming a normalized base, Eqs. (2) and (3) can be rewritten as $\hat{\mathbf{V}} = \mathbf{B}^{\mathrm{T}}\mathbf{A}$ and $\mathbf{A} = \mathbf{B}\mathbf{V}$, respectively. Substitution of (3) into (2) produces $\hat{\mathbf{V}} = \mathbf{B}^{\mathrm{T}}\mathbf{B}\mathbf{V}$. The residue or filtered signal $\mathbf{V}_f$ can be expressed as

$$\mathbf{V}_f = \mathbf{V} - \hat{\mathbf{V}} = (\mathbf{I} - \mathbf{B}^{\mathrm{T}}\mathbf{B})\mathbf{V} = \mathbf{F}\mathbf{V}, \tag{5}$$

where $\mathbf{I}$ is the identity matrix and the regression filter matrix is defined by

$$\mathbf{F} = \mathbf{I} - \mathbf{B}^{\mathrm{T}}\mathbf{B}. \tag{6}$$

The regression filter block diagram is shown in Fig. 1, and from Eq. (5) it is apparent that the filter is linear (matrix multiplication is a linear transformation), time-varying, and responds to the general input–output equation of the form

$$y(t_l) = \sum_{m=0}^{M-1} f(t_l, t_m)x(t_m); \qquad l = 0, \ldots, M-1, \quad (7)$$

where $f(t_l, t_m)$ are the entries of the matrix **F** defined in Eq. (6).

The filter matrix **F** depends only on p and M, so it can be precomputed for real-time applications and does not need to be recomputed if the notch width or sampling scheme do not change. In any case, M need not be equal to the total number of samples M_T in the input signal used to estimate spectral moments. Implementation of regression filters for the case $M_T > M$ is discussed by Torres and Zrnic (1998). Hereafter, to avoid confusion we will use M_f when referring to the length of the regression filter and M_T to indicate the total number of samples in the time series.

The frequency response $H(\omega)$ of a linear shift-invariant system can be defined as the change in magnitude and phase of a complex exponential signal $e^{j\omega t}$, which is passed through the system. More precisely, let $x(t)$ and $y(t)$ be the input and output of the filter whose impulse response is given by $h(t)$. Let $x(t) = e^{j\omega t}$, then the output $y(t)$ can be obtained by convolving $x(t)$ with $h(t)$, that is,

$$y(t) = h(t)^* x(t) = \sum_{t' \in \{t_m\}} h(t')x(t - t') = \sum_{t' \in \{t_m\}} h(t')e^{j\omega(t-t')}$$

$$= \left[\sum_{t' \in \{t_m\}} h(t')e^{-j\omega t'}\right] e^{j\omega t} = H(\omega)e^{j\omega t}, \quad (8)$$

in which $H(\omega)$ describes the frequency response at ω.

As previously stated, the regression filter is time varying. However, the output to a given signal of M_f samples is always the same regardless of when this block of M_f samples is encountered in the filtering process. We will exploit this fact by deriving an expression for the frequency response of the regression filter using Eq. (7) in an analogous fashion as Eq. (8) following the analysis by Torp (1997). That is, consider the regression filter whose input is an exponential of the form $e^{j\omega t}$. The output of this filter is

$$y(t_l) = \sum_{m=0}^{M_f-1} f(t_l, t_m)e^{j\omega t_m}$$

$$= \left[\left(\sum_{m=0}^{M_f-1} f(t_l, t_m)\exp[j\omega t_m]\right)\exp[-j\omega t_l]\right]\exp[j\omega t_l];$$

$$l = 1, \ldots, M_f. \quad (9)$$

Then, by noting the form of (9) we define

$$H(\omega, t_l) = F_l(-\omega)\exp[-j\omega t_l], \quad (10)$$

where $F_l(\omega) = \sum_{m=0}^{M_f-1} f(t_l, t_m)e^{-j\omega t_m}$ is the discrete Fourier transform (DFT) of $f(t_l, t_m)$ with fixed l. Finally, accounting for all the values of l in the M_f sample segment

$$H(\omega) = \frac{1}{M_f}\sum_{l=0}^{M_f-1} F_l(-\omega)\exp[-j\omega t_l]. \quad (11)$$

Using the results of Eq. (6), each entry in **F** is given by

$$f(t_l, t_m) = \delta(t_l - t_m) - \sum_{i=0}^{p} b_i(t_l)b_i(t_m), \quad (12)$$

where $\delta(t)$ is the usual discrete-time impulse sequence. The DFT of (12) is

$$F_l(\omega) = \exp[-j\omega t_l] - \sum_{i=0}^{p} b_i(t_l)B_i(\omega), \quad (13)$$

where $B_i(\omega)$ is the DFT of $b_i(t)$. Then,

$$H(\omega) = 1 - \frac{1}{M_f}\sum_{i=0}^{p} B_i(-\omega)\left[\sum_{l=0}^{M_f-1} b_i(t_l)\exp[-j\omega t_l]\right], \quad (14)$$

and finally the frequency response of the regression filter is given by

$$H(\omega) = 1 - \frac{1}{M_f}\sum_{i=0}^{p} |B_i(\omega)|^2. \quad (15)$$

Note that because $H(\omega)$ is real, the phase response of this filter is constant and we only need to be concerned about its magnitude response. Also, as depicted in Fig. 1, $H(\omega)$ consists of a direct path, the ''1'' in Eq. (15), and a weighted path given by the least squares fit projection, which corresponds to the second term.

The frequency response of the regression filter depends on the number p of elements in B (i.e., the maximum degree of the polynomials used for approximation) and on the number of samples M_f in each processing block. High-frequency signals exhibit rapid changes in time and hence they are better approximated as p increases. Therefore, by increasing p, we allow high-frequency components to be subtracted from the input signal, and this results in a broader notch width. On the other hand, for a fixed p higher frequencies are eliminated if the filter window M_f is shorter. That is, polynomials of a relatively low degree can still ''follow'' high-frequency components if the filter window is ''short.'' Consequently, the notch width of the regression filter increases when M_f decreases. This dependence is illustrated in Figs. 2a and 2b for the uniform PRT scheme. From these plots, we can confirm that the notch bandwidth increases with p and decreases as M_f increases.

The WSR-88D fifth-order elliptic GCF can be programmed for three different suppression levels: low, medium, or high suppression. These selections correspond to notch widths of 2.36 ($\pm$1.18), 3.12 ($\pm$1.56), and 5.06 m s^{-1} ($\pm$2.53 m s^{-1}), which do not change with the number of samples M_T (Chrisman et al. 1995). The steady-state frequency responses of the low, medium, and high suppression fifth-order elliptic GCF for the WSR-88D are also plotted for comparison in Fig. 2

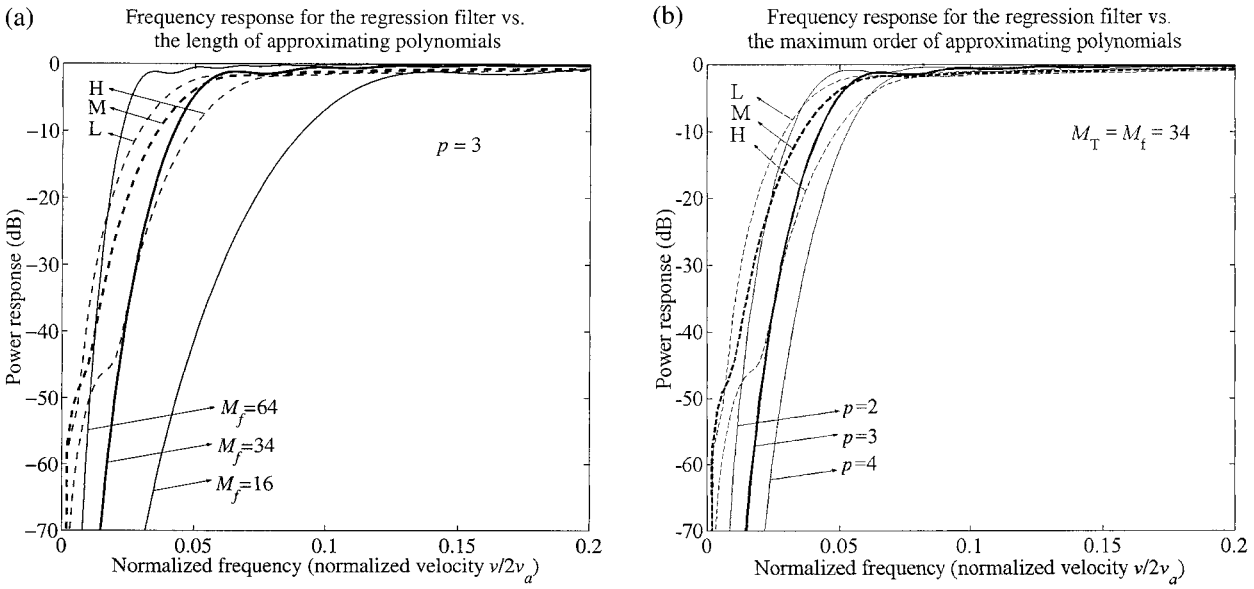

FIG. 2. Regression filter frequency response (solid lines) with (*a*) p and (*b*) M_f as parameters. The frequency responses of the low (L), medium (M), and high (H) suppression fifth-order elliptic filter used in the WSR-88D are also included (dashed lines) for comparison. Two-pulse extension of the step initialization process is used to improve the response of the fifth-order elliptic filter, that is, suppress the transient due to the step inputs at the beginning of pulse bursts for velocity estimation. Bold lines correspond to the filters analyzed in section 4.

(dashed lines). The general form of the transfer function of this filter is

$$H_{\text{WSR-88D}}(z) = \frac{b_0 + b_1 z^{-1} + b_2 z^{-2} + b_3 z^{-3} + b_4 z^{-4} + b_5 z^{-5}}{1 - a_1 z^{-1} - a_2 z^{-2} - a_3 z^{-3} - a_4 z^{-4} - a_5 z^{-5}}, \quad (16)$$

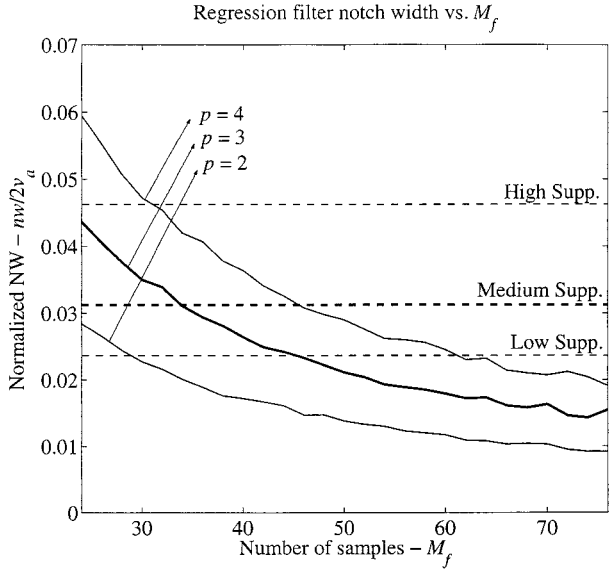

FIG. 3. Regression filter 3-dB notch width vs the number of samples and order of approximating polynomials (solid lines). Notch widths of the WSR-88D filters are indicated with dashed lines. Note that the regression filter with $p = 3$ and the medium suppression WSR-88D ground clutter filter have matched notch widths for $M_f = 34$. These two filters (bold lines) are compared in section 4.

where the coefficient a_i's and b_i's are obtained from the classical design formulas for digital elliptic filters, as given in Parks and Burrus (1987).

During scans at elevation angles larger than 1.5° the WSR-88D transmits an interlaced waveform whereby a batch of short PRTs is for Doppler measurements. To achieve the indicated frequency response, the GCF uses a two-pulse extension of the *step initialization* process, as described by Sirmans (1992). This process consists of setting the filter memories to steady state, assuming a DC clutter signal with amplitude equal to the first pulse in the batch. For this analysis, we adopt the number of samples $M_T = 34$ in the input signal. An increase in the number of samples causes a sharper notch, which tends to the theoretical steady-state response of (16). In the WSR-88D, the actual number of samples in a radial depends on the volume coverage pattern (VCP) mode and can be from 33 to 111 samples. Therefore, the adopted $M_T = 34$ represents a worst-case filter fitting scenario.

Figure 3 shows how the filter's 3-dB notch width depends on the number of samples for both classes of GCFs. As a useful tool for further comparison, we find a direct equivalence between each suppression level of the fifth-order elliptic filter and the order of approximating polynomials in the regression filter. Observe, for instance, that for $p = 3$ and $M_f = 34$, the notch width of the regression filter matches that of the medium suppression GCF in the WSR-88D. However, the regression filter achieves a sharper transition region. In section 4, we compare the two filters having this matching condition.

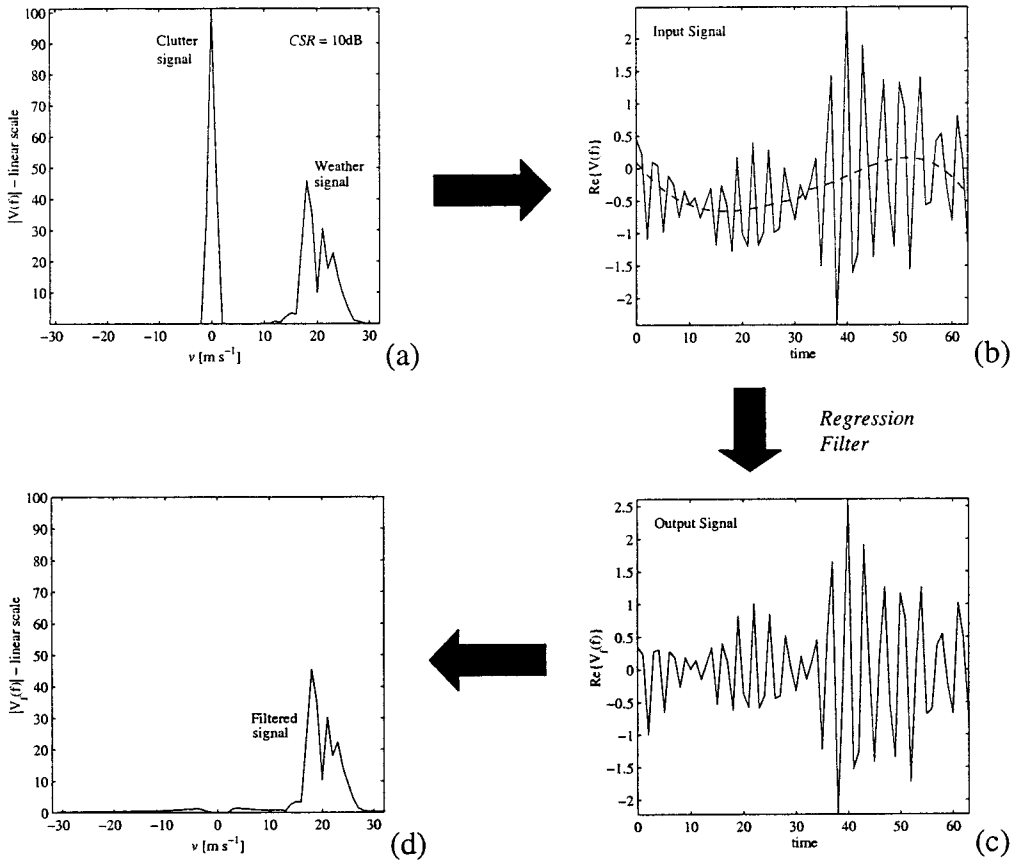

FIG. 4. Clutter filtering process with a regression filter. (a) Spectrum of a weather signal contaminated with ground clutter. (b) Time-domain representation of the composite signal. The dashed line is the third-order polynomial fit to this signal, that is, the estimated clutter. (c) Filtered signal in the time domain used to determine the three fundamental physical parameters (mean power, mean Doppler velocity, and spectrum width). (d) Spectrum of the filtered signal.

The regression filter has several attractive properties compared to the GCF currently implemented in the WSR-88D. While the latter is greatly influenced by the filter's transient response characteristics, the regression filter inherently avoids these transients (i.e., these filters do not cause transients). Moreover, regression filter's design methods diverge from the ones used with classical filters because their implementation consists of a matrix multiplication instead of a set of equations evaluated recursively at each time step. Thus, regression filters are well suited for modern array processors.

3. Performance analysis of the regression filter

In this section, we describe a series of simulations to establish the performance of the regression filter and compare the results with the fifth-order elliptic GCF implemented in the WSR-88D. The clutter signal is modeled as a narrowband Gaussian process with zero mean velocity. This clutter and white noise are added to a synthetic weather signal (Zrnic 1975). Then, the composite signal is filtered to remove the ground clutter, and finally the first three moments of the weather Doppler spectrum are estimated using the classical pulse pair algorithm. This process is shown in Fig. 4.

Two parameters of interest for these simulations are the signal-to-noise ratio (SNR) and the clutter-to-signal ratio (CSR), which are defined as SNR (dB) = 10 $\log_{10}(S/N)$ and CSR (dB) = 10 $\log_{10}(C/S)$, where S, C, and N are signal, clutter, and noise powers, respectively. The clutter filter suppression ratio (CFSR), a measure of the filter's performance, is defined by

$$\text{CFSR (dB)} = 10 \log_{10}(G_{\text{noise}}^{-1} P_{\text{out}}/P_{\text{in}}). \qquad (17)$$

In this equation P_{in} and P_{out} are the powers measured at the input and output of the filter, respectively, and G_{noise} is the noise gain of the filter defined by $P_{\text{out}}/P_{\text{in}}$ when the input to the filter is white noise. Note that G_{noise} depends only on the frequency response of the filter, and for the regression filter can be computed by using (15). The CFSR in the absence of weather signal of both the regression filter and the WSR-88D elliptic filter (described in section 2) is depicted in Fig. 5. Note that for the most common case of narrow clutter spectrum

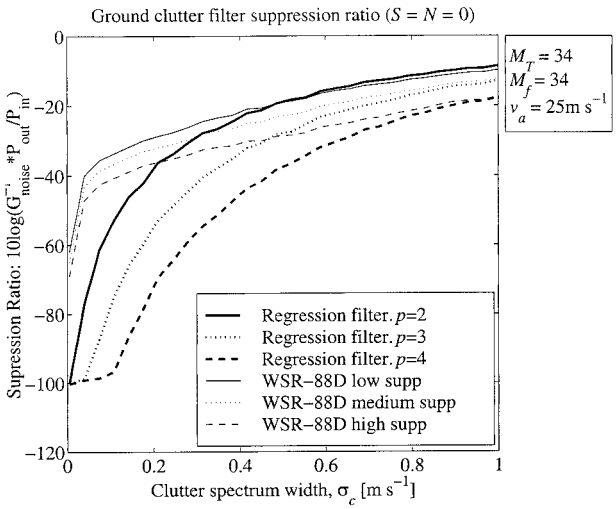

FIG. 5. Clutter suppression ratio vs the clutter signal spectrum width. Solid lines correspond to regression filters for different values of p and dashed lines to the elliptic filters (low, medium, and high suppression) implemented in the WSR-88D.

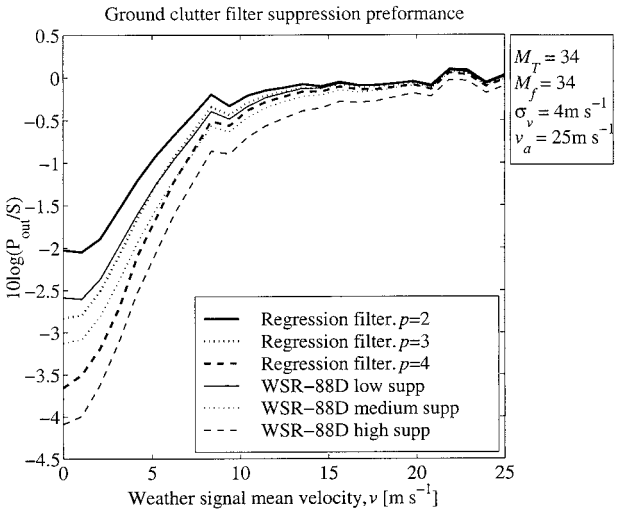

FIG. 6. Suppression ratio for the weather signal vs its mean velocity. Here, $\sigma_v = 4$ m s^{-1} (median value in severe storms). Solid lines correspond to regression filters for different values of p and dashed lines to the elliptic filters (low, medium, and high suppression) implemented in the WSR-88D.

widths (i.e., $\sigma_c < 0.5$ m s^{-1}), the suppression ratio of the regression filter with $p = 4$ is at least 10 dB better than the one achieved by the high-suppression elliptic GCF. In general, the regression filter performs better than the comparable elliptic filter, especially if the spectrum width of the clutter is very narrow.

The suppression of weatherlike signals, by these filters, is plotted in Fig. 6, where the mean velocity changes from 0 to 25 m s^{-1} and the spectrum width is set at 4 m s^{-1}, which is the median found in severe storm observations (Doviak and Zrnic 1993). Over 1 dB of suppression is observed for signal mean velocities below 4.5–6.5 m s^{-1}, depending on the notch width of the filter. At that, performances of regression filters are comparable to the elliptic filters of corresponding notch width. Similar results hold for weather signals with spectrum width of 1 m s^{-1} (typical of stratiform rain) except the 1-dB suppression is for velocities below 3–5 m s^{-1}. These curves (Fig. 6) indicate the power estimation biases one can expect if the mean velocity of the weather signal is close to zero. However, when the mean velocity of the weather signal is well away from 0 m s^{-1}, neither filter biases the power estimates.

For a more realistic situation, a weather signal was combined with the ground clutter and the ratio P_{out}/S was computed for different CSRs. This analysis is shown in Fig. 7 for a CSR of 20 dB. The clutter spectrum width is set at 0.28 m s^{-1}, which is the same as the one used for testing the WSR-88D ground clutter filter performance (Sirmans 1992). Measurements on the WSR-88D in Norman, Oklahoma, indicate that the mean of clutter spectrum width is 0.25 m s^{-1} for a scan rate of 12° s^{-1}; therefore, 0.28 m s^{-1} is in the worst-case category. Figure 7 confirms that the reflectivity estimates can have a significant negative bias if the mean Doppler velocity of the weather signal is such that its spectrum overlaps the one of the ground clutter. In addition, we observe a small positive bias (WSR-88D low suppression) if the mean Doppler velocity departs from the origin because the clutter signal is not fully removed by the elliptic filter. For the CSR of 40 dB (not shown), we found that the elliptic GCF does not remove the clutter signal completely, leaving an almost constant bias along the entire velocity range. Similar bias was present for the second-order regression filter, but the fourth-order regression filter had no bias. Evidently, this

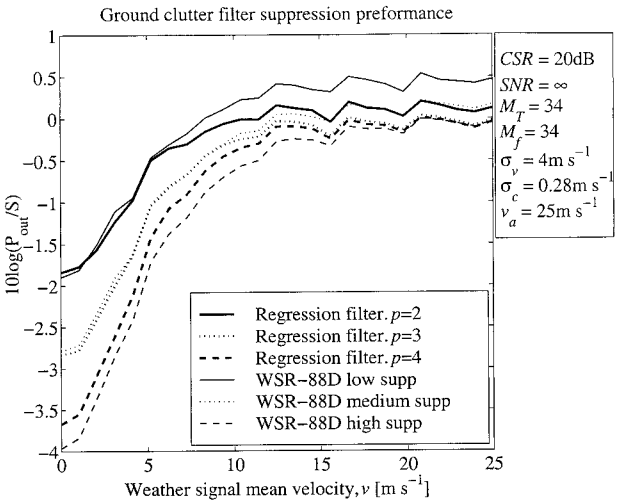

FIG. 7. Suppression ratio of regression and elliptic GCFs vs weather signal mean velocity for a CSR of 20 dB. Solid lines correspond to regression filters for different values of p and dashed lines to the elliptic filters (low, medium, and high suppression) implemented in the WSR-88D.

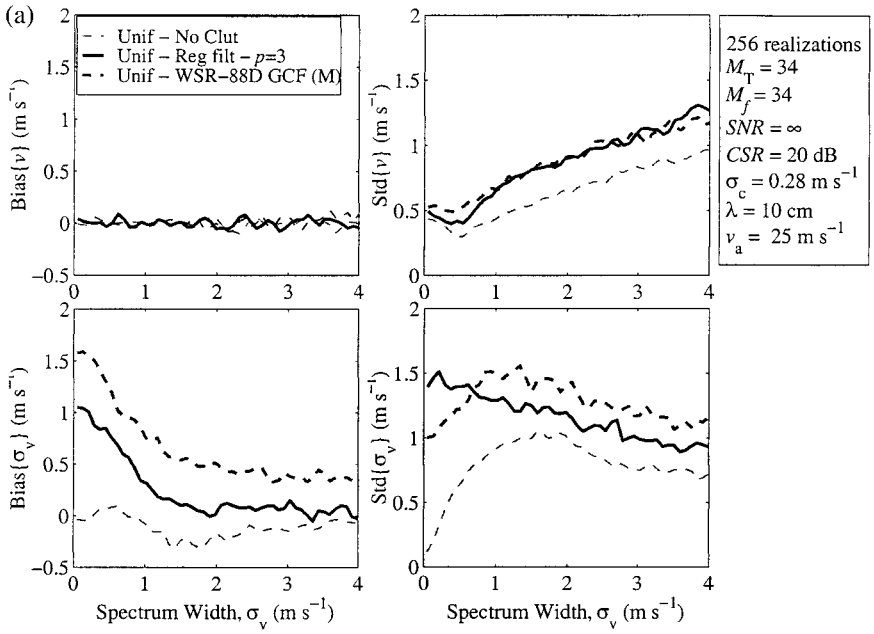

FIG. 8. Pulse-pair algorithm statistical performance: bias and standard deviation of mean Doppler velocity and spectrum width estimates (a) vs the weather signal mean velocity and (b) vs the weather signal spectrum width. Parameters for the simulation are indicated in the figure. Solid lines

effect gets worse for larger CSR and wider clutter spectrum width, but it can be controlled by adjusting the ground clutter filter frequency response.

As the ultimate goal is to accurately recover the three first spectral moments of the weather signal, the pulse pair statistical performance for different CSRs was computed versus (i) the weather signal spectrum width and (ii) the weather signal mean velocity for both regression and elliptic WSR-88D filters. Consider first the case where the weather signal mean velocity is a parameter and the spectrum width is randomly selected from the interval (2, 6) m s^{-1} (Fig. 8a). Then, there are large positive biases in both the mean velocity and the spectrum width estimates if the true mean velocity of the weather signal is less than approximately 5 m s^{-1}. This is due to overlap of the weather spectra and clutter notch. A part of the spectrum close to zero velocity is eliminated by the filter; therefore, the nonfiltered components bias the velocity upward. Mean velocity bias for the regression filter is about 0.25 m s^{-1} larger than for the elliptic filter at $v < 10$ m s^{-1}. The standard deviations of the velocity estimates are comparable and very close to the performance of the pulse-pair algorithm in the absence of clutter. The bias and standard deviation of spectrum widths are smaller (at $v > 8$ m s^{-1}) for the regression filter.

Next, we take the weather-signal spectrum width as a parameter and randomly select its mean velocity from the interval (−25, 25) m s^{-1} (Fig. 8b). Notice that variations in the mean velocity bias and the standard deviation increase with the weather-signal spectrum width. This effect is consistent with the algorithm performance and slightly more evident if there is contamination by the clutter signal. This is because the weather signal extends over a larger portion of the spectrum and it is more likely to be adversely shaped by the ground clutter filter. The bias in v and the standard deviations for the two filters are comparable. A slightly smaller bias and standard deviation are seen for the regression filter. Because the GCF does not remove the clutter signal completely, for small spectrum widths, we observe a positive bias in the spectrum width estimates, which increases with the CSR. From these figures, we conclude that influences of the regression filter and the corresponding elliptic filter on the statistical performance of pulse-pair estimators are comparable.

4. Application of filters to the WSR-88D data

Time series data (i.e., I and Q samples) have been collected from a WSR-88D in Memphis at the lowest elevation of 0.5°, while the antenna was scanning at 12° s^{-1}. Sixty-four samples of the in-phase component (Fig. 9a) reveal a slowly varying clutter signal and possibly weak weather signal. The Doppler spectrum (Fig. 9b) has a peak at zero, which is 75 dB above the receiver noise level. This large spectral dynamic range has been routinely observed on both Memphis and Norman WSR-88D and testifies to the very high quality of the system. The spectrum width of this ground clutter is 0.23 m s^{-1}, the CSR is 33 dB and the SNR is 26 dB.

Figure 10 shows the signals produced by application of the regression filter with $p = 3$ (solid lines) and the ''medium suppression'' elliptic filter (dashed lines). The

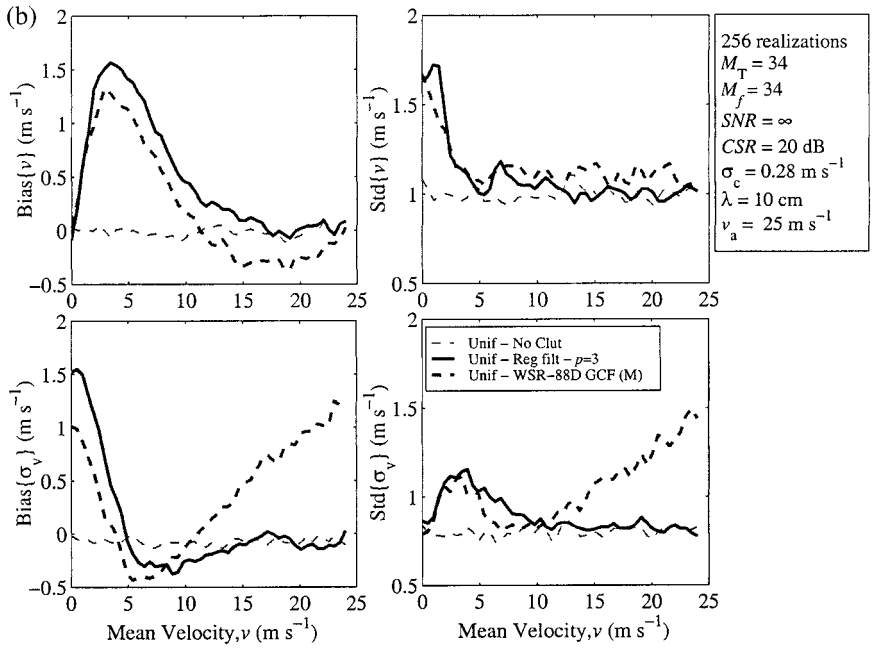

FIG. 8. (*Continued*) correspond to the regression filters for $p = 3$ and dashed lines to the medium-suppression elliptic filter implemented in the WSR-88D.

regression filter with $M_f = 34$ is applied to the 64 input samples similar to a moving average filter. Note how the in-phase signal after regression filtering has no discernible slow varying component, whereas after filtering with the elliptic filter it does. This is also reflected in the spectral shapes at and close to zero velocity. The clutter spectrum has been suppressed at least 40 dB below the weather peak after application of the regression filter (Fig. 10b, solid line) and it is slightly above the weather peak after application of the elliptic filter (Fig. 10b, dashed line). Note that although the notch widths of the two filters are matched, it is the response in the transition region of the regression filter that makes it the better of the two.

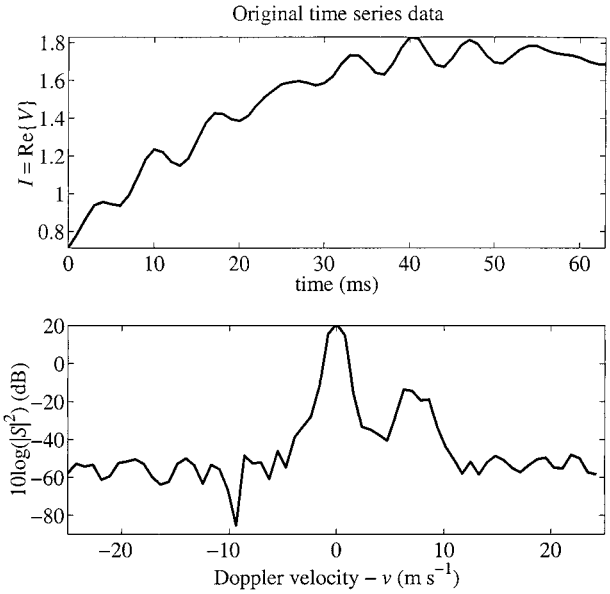

FIG. 9. Data collected with the WSR-88D in Memphis at an elevation of 0.5° and a range of 15 km. (a) In-phase component and (b) Doppler spectrum of the time series to which the von Hann window has been applied.

5. Conclusions

We have explored the suitability of regression filters for ground clutter suppression in Doppler weather radars. First, a brief review of how to design these filters and determine the frequency response was presented. Parameters that control the frequency response are the number of samples to which regression is applied and the degree of the regression polynomial. The increase in the polynomial degree (p) broadens the filter's notch width because higher frequencies are subtracted from the signal. The notch width also broadens if the number of samples (M_f) decreases because then the regression polynomial better replicates high frequency components. Different families of approximating polynomials only affect the computational complexity of the implementation, which is considerably reduced if this set is orthonormal. Regression filters are easy to implement and do not require initialization such as is needed in the Doppler mode of data processing at higher than 1.5° in elevation on the WSR-88D. Preliminary studies and simulations indicate that the suppression characteristics of regression filters meet or exceed those of step-initialized IIR filters (with matched notch width), in which

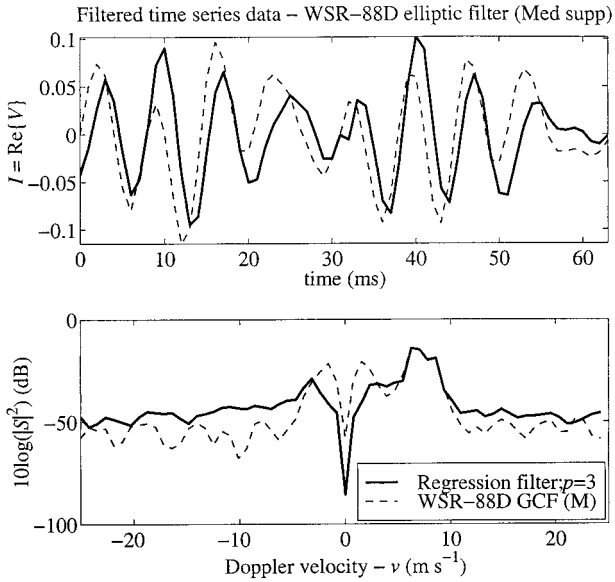

FIG. 10. Time series data filtered with the medium-suppression regression filter ($p = 3$, solid line) and filtered with the medium suppression WSR-88D ground clutter filter (dashed line). (a) In-phase filtered component and (b) Doppler spectrum of the filtered signal (weighted with the von Hann window).

transients degrade the theoretical frequency response. For $p = 3$ and $M_f = 32$, the regression filter approximates the statistical performance of the medium-suppression fifth-order elliptic filter in the WSR-88D. Comparison of the two filters (with matched notch width) on an actual weather signal, collected by an operational WSR-88D, indicates that the regression filter performs better. This is due to the superior shape of the regression filter's frequency response in the cutoff region.

Acknowledgments. The authors appreciate suggestions by R. J. Doviak, which have improved the paper. The Memphis data were collected and supplied by C. Frush, D. Ferraro, and J. VanAndel. This work was supported by the Operations Support Facility of the National Weather Service. In addition, the helpful comments of the reviewers and Dr. R. Strauch are gratefully acknowledged.

REFERENCES

Chrisman, J. N., D. M. Rinderknecht, and R. S. Hamilton, 1995: WSR-88D clutter suppression and its impact on meteorological data interpretation. Postprints, *The First WSR-88D User's Conf.*, Norman, OK, WSR-88D Operational Support Facility and NEXRAD Joint System Program Office, 9–20.

Doviak, R. J., and D. Zrnic, 1993: *Doppler Radar and Weather Observations.* 2d ed. Academic Press, 562 pp.

Egecioglu, O., and C. Koc, 1992: A parallel algorithm for generating discrete orthogonal polynomials. *Parallel Computing,* **18,** 649–659.

Heiss, W., D. McGrew, and D. Sirmans, 1990: NEXRAD: Next Generation Weather Radar (WSR-88D). *Microwave J.,* **33,** 79–98.

Hoeks, A. P., J. J. van-de-Vorst, A. Dabekaussen, P. J. Brands, and R. S. Reneman, 1991: An efficient algorithm to remove low frequency Doppler signals in digital Doppler systems. *Ultrason. Imag.,* **13,** 135–44.

Kadi, A. P., and T. Loupas, 1995: On the performance of regression and step-initialized IIR clutter filters for color Doppler systems in diagnostic medial ultrasound. *IEEE Trans. Ultrason., Ferroelect., Freq. Control,* **42,** 927–937.

May, P. T., and R. G. Strauch, 1998: Reducing the effect of ground clutter on wind profiler velocity measurements. *J. Atmos. Oceanic Technol.,* **15,** 579–586.

Papoulis, A., 1986: *Signal Analysis.* 3d ed. McGraw-Hill, 431 pp.

Parks, T. W., and C. S. Burrus, 1987: *Digital Filter Design.* John Wiley and Sons, 342 pp.

Sirmans, D., 1992: Clutter filtering in the WSR-88D. NWS/OSF Internal Rep., 125 pp. [Available from National Weather Service Operational Support Facility, 1200 Weistheimer Dr., Norman, OK 73069.]

Torp, H., 1997: Clutter rejection filters in color flow imaging: Atheoretical approach. *IEEE Trans. Ultrason., Ferroelect., Freq. Control,* **44,** 417–424.

Torres, S., and D. Zrnic, 1998: Ground clutter canceling with a regression filter. NSSL Interim Rep. 35 pp. [Available from Doppler Radar and Remote Sensing Group, National Severe Storms Laboratory, 1313 Halley Circle, Norman, OK 73069.]

Zrnic, D., 1975: Simulation of weatherlike Doppler spectra and signals. *J. Appl. Meteor.,* **14,** 619–620.